Cancer Management and Research

Elevate Series

Open Access Full Text Article

ORIGINAL RESEARCH

Cytotoxic Effect of *Halimeda macroloba* Crude Extract on Cervical Cancer Spheroid Cells via p-mTOR/mTOR, Apoptosis, and Ferroptosis Pathways

Kesara Nittayaboon[1], Kittinun Leetanaporn[1,2], Kankamol Kerdkumthong[1], Jaruwan Mayakun[3], Raphatphorn Navakanitworakul[1,2]

[1]Department of Biomedical Sciences and Biomedical Engineering, Faculty of Medicine, Prince of Songkla University, Hat Yai, Songkhla, 90110, Thailand; [2]Translational Medicine Research Center, Faculty of Medicine, Prince of Songkla University, Hat Yai, Thailand; [3]Division of Biological Science, Faculty of Science, Prince of Songkla University, Hat Yai, Songkhla, 90110, Thailand

Correspondence: Jaruwan Mayakun, Department of Biomedical Sciences and Biomedical Engineering, Faculty of Medicine, Prince of Songkla University, Hat Yai, Songkhla, 90110, Thailand, Email jaruwan.may@psu.ac.th; Raphatphorn Navakanitworakul, Division of Biological Science, Faculty of Science, Prince of Songkla University, Hat Yai, Songkhla, 90110, Thailand, Email nraphatp@medicine.psu.ac.th

Background: Because of the limited efficacy of existing therapeutic strategies and the emergence of treatment resistance, cervical cancer remains a major global health burden. Recently, marine-derived natural compounds have attracted attention as potential sources of novel anticancer agents. We aimed to investigate the cytotoxic effects of crude *Halimeda macroloba* extract on cervical cancer spheroid cells and to explore its underlying molecular mechanisms.

Methods: Three-dimensional spheroid cultures of SiHa cervical cancer cells were treated with varying concentrations of *H. macroloba* extract, followed by assessment of migration, cell viability, caspase activity, and protein expression profiles using liquid chromatography–tandem mass spectrometry, with selected findings validated by Western blotting.

Results: Treatment with *H. macroloba* extract significantly reduced spheroid migration and decreased cell viability in a dose-dependent manner, accompanied by increased caspase activity. Proteomic analysis demonstrated altered expression of proteins associated with mitochondrial function, apoptosis-related pathways, and oxidative stress-related processes. Mechanistic studies further revealed down-regulation of phosphorylated mTOR (p-mTOR) and total mTOR, together with increased expression of pro-apoptotic markers.

Conclusion: The *H. macroloba* crude extract exerts anticancer effects in cervical cancer spheroids, primarily through apoptosis-associated mechanisms and modulation of the mTOR signaling pathway, supporting its potential for further investigation as a marine-derived bioactive compound.

Keywords: cervical cancer, natural extracts, proteomic analysis, anticancer agents

Introduction

Natural products exhibit a wide range of biological properties beneficial for medical applications. These compounds are being increasingly recognized as crucial contributors to drug discovery and development. Among them, the marine calcified green seaweed, *Halimeda* (J. V. Lamouroux), belonging to the Halimedaceae family, Bryopsidales order, and Bryopidopyceae class, has emerged as a promising candidate for biomedical research. *Halimeda* is broadly distributed across tropical and subtropical regions and is abundant in numerous reef systems such as the Florida Keys, Southwest Atlantic Ocean, and Indo-Pacific Ocean.[1–6] In Thailand, *Halimeda macroloba* is particularly abundant in the shallow subtidal and intertidal zones, and forms dense populations in the intertidal zone of Lidee Island, Satun Province.[7] *H. macroloba* is an important calcium carbonate producer that contributes to the carbonate budget.[8,9] *Halimeda* produces hydrocolloids, which are utilized in both the food and pharmaceutical industries, thereby making it economically relevant. Furthermore, *Halimeda* is a rich source of bioactive compounds including carotenoids, xenicane lactones, sym-triazine derivatives, bis-indole alkaloids, bis-nor diterpene derivatives, phenolics, flavonoids, terpenoids, and polysaccharides. This species also exhibits high phenolic and flavonoid content, contributing to its strong antioxidant

https://doi.org/10.2147/CMAR.S611650
Received: 25 March 2026
Accepted: 3 July 2026
Published: 10 July 2026

potential. These secondary metabolites display diverse pharmacological activities including antioxidant, anticancer, anti-inflammatory, antimicrobial, and antiviral properties.[2,10]

Cervical cancer is the fourth most prevalent cancer in women worldwide. Breast cancer is the second most common type of cancer in Thailand. The introduction of screening programs and human papilloma virus (HPV) vaccination has contributed to a reduction in incidence rates.[11] Standard treatment options for cervical cancer include surgery, radiotherapy, chemotherapy, and combined chemoradiotherapy.[11,12] However, the mortality rate associated with cervical cancer in Thailand has increased, thereby indicating a critical gap in research and intervention. Natural compounds represent a major source of clinically approved anticancer agents and continue to serve as a critical reservoir for oncologic drug discovery.[13] The potential therapeutic activity of *Halimeda* has been reported in various cancer types, including cervical cancer.[10] However, the chemical composition of *Halimeda* varies depending on environmental conditions and nutrient availability across different geographical regions. Despite the reported bioactive properties of *Halimeda* species, the anticancer effects and underlying molecular mechanisms of *H. macroloba* in cervical cancer remain poorly understood, particularly in physiologically relevant 3D tumor models. Three-dimensional spheroid cultures more closely mimic the tumor microenvironment, including cell–cell interactions, nutrient gradients, hypoxic regions, and drug penetration characteristics observed in solid tumors, thereby providing a more predictive platform for evaluating anticancer activity than conventional 2D monolayer cultures.[14] In addition, growing evidence suggests that marine-derived natural compounds may modulate oxidative stress and lipid peroxidation-associated pathways, including ferroptosis-related mechanisms, which have emerged as potential therapeutic targets in cancer treatment. However, the possible involvement of ferroptosis-associated pathways in the anticancer effects of *H. macroloba* has not yet been investigated.

In this study, we aimed to investigate the cytotoxic effects of *H. macroloba* extract on cervical cancer spheroids and explored the associated molecular mechanisms, including apoptosis- and ferroptosis-related pathways. Figure 1 shows the research workflow.

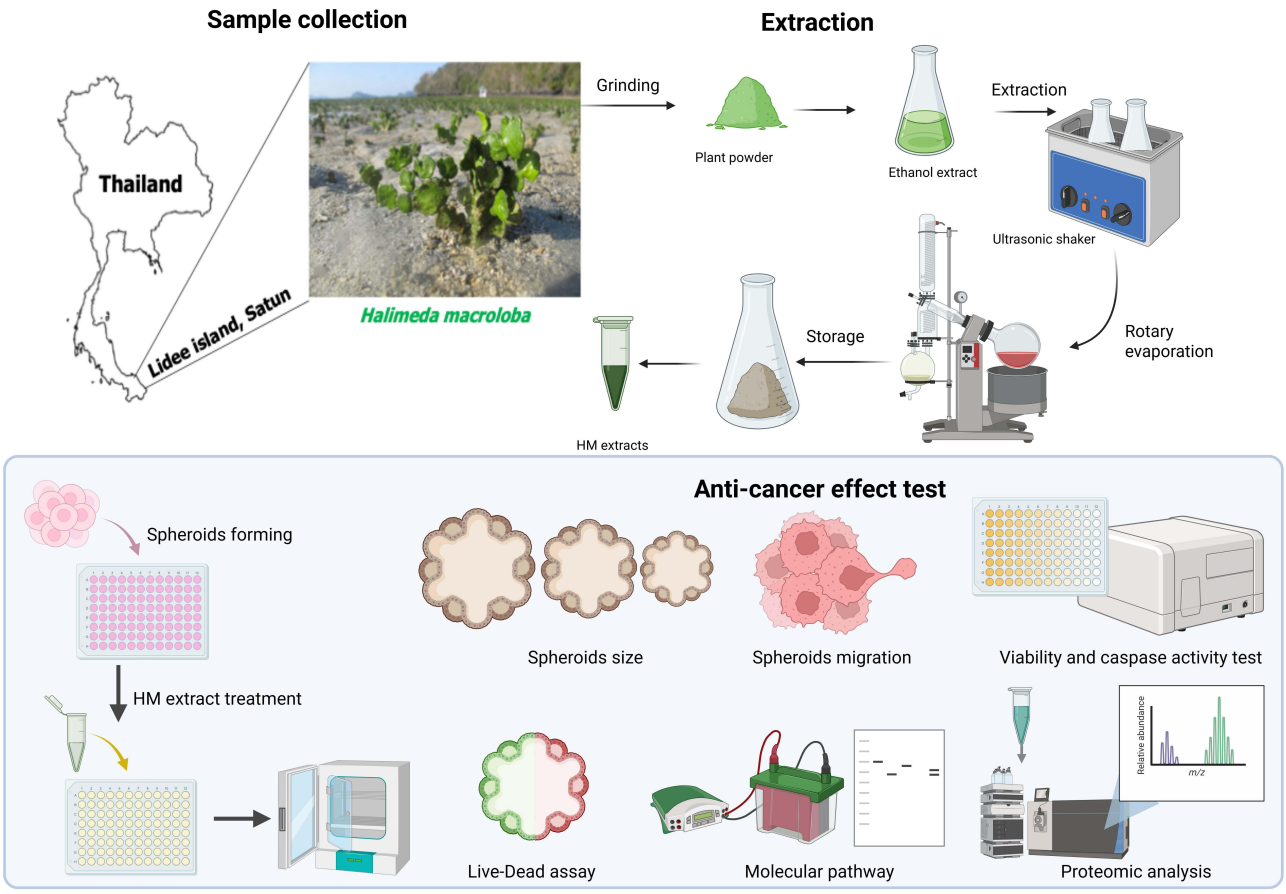

Figure 1 Research workflow. The upper and lower panels illustrate the crude extract preparation process, including sample collection and extraction step, and anticancer testing procedure, respectively.

Materials and Methods

Cervical Cancer Cell Culture and Spheroid Culture

A squamous cell carcinoma of cervical cancer cells, SiHa (ATCC HTB-35), was purchased from the American Type Culture Collection (ATCC) (Manassas, VA). The cells were cultured in Dulbecco's Modified Eagle's Medium (DMEM, Gibco, Thermo Fisher Scientific, USA) supplemented with 10% fetal bovine serum (FBS, Gibco, Thermo Fisher Scientific, USA), L-glutamine, streptomycin (100 µg/mL, Gibco, Thermo Fisher Scientific, USA), and penicillin (100 U/mL, Gibco, Thermo Fisher Scientific, USA), and incubated in humidified air with 5% CO2 incubator at 37 °C.

Spheroid cells were grown on poly-(2-hydroxyethyl methacrylate)-or poly HEMA-coated plates (Sigma-Aldrich, USA). The low-attachment plates were prepared by transferring an aliquot of 20 µL of Poly-HEMA working solution (5 mg/mL) into a single well of a 96-well U-bottom plate (Thermo Fisher Scientific, USA). Subsequently, the plates were dried in an incubator for 3 days. SiHa cells were seeded into the plates at a density of 5000 cells/well in 10% FBS-DMEM complete medium to generate spheroid cells.[14]

H. macroloba Extract Preparation

H. macroloba extracts were prepared and subjected to phytochemical analysis. Briefly, *H. macroloba* was dried, ground, extracted with ethanol, and concentrated under reduced pressure. Phytochemical screening and thin-layer chromatography were performed as previously described.[7] The major identified bioactive constituents included alkaloids, flavonoids, phenolic compounds, terpenoids, steroids, and saponins. For cytotoxicity assays, the extracts were dissolved in dimethyl sulfoxide (DMSO).

Spheroid Size and Migration Evaluation

Spheroid size was evaluated using three independent biological replicates, with each replicate containing three spheroids per condition. Spheroids were imaged on day 3 following treatment with *H. macroloba* extract, and spheroid diameters were measured using ImageJ software (version 1.54). The average spheroid diameter was calculated and compared among treatment groups. For the spheroid migration assay, spheroids were collected on day 3 post-treatment and transferred to flat-bottom plates containing fresh complete medium. The spheroids were further incubated for 72 h to allow cell migration. Migration areas were subsequently imaged and quantified using ImageJ software. Both spheroid diameter and migration area were analyzed quantitatively.

Cytotoxicity Test

Cell viability and cytotoxicity were evaluated following a 3-day treatment with *H. macroloba* extract using a LIVE/DEAD Cell Imaging Kit (Thermo Fisher Scientific, USA). Experiments were performed using three independent biological replicates, each consisting of three spheroids per treatment condition. Calcein AM was used to identify viable cells, whereas BOBO-3 iodide was used to detect dead cells. Prior to staining, the culture medium volume was adjusted to 30 µL. Following incubation with the staining solution at 37 °C for 30 min in the dark, fluorescence images were acquired using a Lionheart FX live-cell imaging system.

The mode of cell death was further characterized following a 3-day treatment using the ApoLive-Glo™ Multiplex Assay (Promega, WI, USA). The assay was performed using three independent biological replicates, each containing three spheroids per condition. This assay simultaneously measures protease activity in viable cells through fluorescence-based detection and caspase-3/7 activity in apoptotic cells via luciferase-based luminescence.

Proteomic Analysis Using Liquid Chromatography Tandem Mass Spectroscopy (LC–MS/MS)

Proteomic analysis was conducted to evaluate protein expression following *H. macroloba* extract treatment. Spheroids with and without treatment were collected in three independent passages, and proteins were extracted using a filter-aided sample preparation (FASP) protocol with minor modifications.[15] In brief, 50 µg of protein was diluted in 50 mM Tris-HCl buffer (pH 8.0) containing 4% sodium dodecyl sulfate (SDS) and heated at 95 °C for 5 min. Thereafter, the samples were washed thrice with 8 M urea in 5 mM Tris-HCl and incubated with 5 mM DTT at 37 °C for 60 min, followed by 15 mM IAA at 25 °C for 30 min, and washed thrice with NH_4CO_3. Protein digestion was conducted using trypsin at a 50:1

(protein: enzyme, w/w) ratio in 50 mM NH_4CO_3 at 37 °C overnight. The reaction was quenched with 1% formic acid (FA), and peptides were desalted using ZipTip (Sigma Aldrich) prior to LC-MS/MS analysis.

For LC–MS/MS analysis, protein samples were analyzed using a Vanquish Neo UHPLC system (Thermo Fisher Scientific, USA) coupled with an Orbitrap Exploris 480 mass spectrometer (Thermo Fisher Scientific). Tryptic digest (1 μg) was loaded onto an Acclaim PepMap C18 trap column (5 μm, 300 μm × 5 mm), followed by peptide separation on a PepMap C18 analytical column (2 μm, 75 μm × 500 mm) at a flow rate of 0.3 μL/min with an electrospray voltage of 2 kV. Chromatographic separation was achieved using a linear gradient from 2% to 45% solvent B (solvent A: 2% acetonitrile with 0.1% formic acid; solvent B: 80% acetonitrile with 0.1% formic acid) for 70 min, and was followed by a 5-min wash with 95% solvent B. The column was maintained at 60 °C throughout the experiments. MS1 scans were acquired within an m/z range of 400–1000 at a resolution of 120,000 with an automatic gain control (AGC) target of 300%. MS2 spectra were generated using data-independent acquisition (DIA) with optimized isolation windows. DIA settings included 20 m/z isolation windows, a resolution of 30,000, an AGC target of 1000%, and a normalized collision energy of 28% using high-energy collisional dissociation.

For data processing, raw spectral files were analyzed using the DIA-NN version 1.9.2.[16] The data were searched against the UniProt Homo sapiens proteome (UP000005640) with the following parameters: allowance for one missed cleavage, N-terminal methionine excision, carbamidomethylation of cysteines as a fixed modification, generic scoring, MS1 and MS2 mass accuracies set to 20 ppm and 10 ppm, respectively, retention time (RT)-time-dependent normalization, high-precision quantification strategy, and match-between-runs functionality. Precursor and protein identification were filtered using a 1% false discovery rate.

For data analysis, proteins detected in fewer than 50% of samples were excluded from further analyses. The remaining missing values were imputed using the Minimal Detection Value method in the *imputeLCMD* package of R. Additionally, protein expression patterns were visualized using heat maps (MetaboAnalyst). The number of proteins expressed in the treatment and control groups was visualized using Venn diagrams (ref WebBase). Differential expression was determined using the *limma package*. Consequently, proteins were classified as differentially expressed when meeting the thresholds of $p < 0.05$ and fold change > |1.5|. Finally, upregulated and downregulated proteins were classified using PANTHER (Protein ANalysis THrough Evolutionary Relationships), and gene enrichment was performed with the *clusterProfiler* package in R for molecular function (MF) and biological process (BP) categories using Fisher's exact test with Benjamini–Hochberg correction ($p < 0.2$).

Molecular Mechanism of H. macroloba Extract Active Compounds

Western blot analysis of spheroids was performed as previously described.[14] Briefly, spheroid pellets collected from three independent passages, with each passage containing nine spheroids, were lysed in radioimmunoprecipitation assay (RIPA) buffer (Pierce Biotechnology, Waltham, MA, USA). The protein concentration was measured using the Bradford assay (Bio-Rad, USA). A total of 30 μg of protein extract was subjected to SDS-polyacrylamide gel electrophoresis (SDS-PAGE), followed by transfer to polyvinylidene difluoride membranes (Amersham Pharmacia Biotech, USA). The membranes were blocked in 5% nonfat milk in Tris-buffered saline containing 0.1% (v/v) Tween-20 (TBS-T) for 1 h at room temperature. The cells were then washed twice with TBS-T for 10 min. Each membrane was incubated overnight at 4 °C, while shaking continuously with primary antibodies (1:1000 diluted with 1% non-fat milk in TBS-T) specific to Akt (cat. no. 4691; Cell Signaling Technology, Inc)., phospho-AKT (Ser473; cat. no. 4060; Cell Signaling Technology, Inc)., phosphorylated mTOR (Ser2448; cat. no. 5536; Cell Signaling Technology, Inc)., USA), mTOR (cat. no. 2983; Cell Signaling Technology, Inc., Danvers, MA, USA), cRaf (cat. no. 9421; Cell Signaling Technology, Inc)., Bax (cat. no. 2772; Cell Signaling Technology, Inc)., cleavage-caspase 3 (cat. no. 9664; Cell Signaling Technology, Inc)., cytochrome C (cat. no. 4272; Cell Signaling Technology, Inc)., and β-actin (cat. no. 4967; Cell Signaling Technology) were used as internal control. After incubation, the membranes were washed thrice (10 min/wash) with TBS-T and incubated with a secondary antibody (Anti-rabbit IgG horseradish peroxidase; cat. no. 7074; Cell Signaling Technology, Inc)., at 1:1000 diluted in 1% nonfat milk in TBS-T for 2 h. Thereafter, the membranes were again washed three times with TBS-T, and the last washing was performed using TBS for 10 min. Protein expression was visualized using an enhanced chemiluminescence reagent (Pierce ECL Western Blotting Substrate, Thermo Fisher Scientific, USA). Densitometry was performed using a Chemiluminescence & Epi Fluorescence Alliance Q9 Advanced Imager (UVITEC, UK).

Statistical Analysis

Statistical analyses were performed using the GraphPad Prism Software (version 9.00; GraphPad, San Diego, CA, USA). Student's *t*-test (two-tailed) was used to compare two independent group means, whereas one- or two-way ANOVA (followed by Tukey's or Sidak's multiple comparison tests) was used to compare more than two independent group means. A p-value < 0.05 were considered statistically significant.

Results

H. macroloba Extracts Inhibited Cervical Cancer Spheroid Migration but Not Spheroid Size

Prior to investigating the anticancer activity of *H. macroloba* extract, its safety profile was evaluated in non-cancerous cells using a 2D monolayer culture model. The extract exhibited minimal cytotoxicity toward L929 fibroblast cells, with an IC_{50} value exceeding 80 µg/mL. Similar findings were observed in HEK-293 cells in our previous study, where the IC_{50} value was also greater than 80 µg/mL.[7] These results indicate a favorable preliminary safety profile and supported the subsequent evaluation of the extract in cervical cancer cell models. The corresponding data are provided in Supplementary Table S1.

Following confirmation of its preliminary safety profile, the effects of *H. macroloba* extract on spheroid morphology and migration were investigated. The morphology of the spheroids was captured after treatment with *H. macroloba* extract. The extracts showed anti-migration activity in spheroids, while spheroid size remained unaffected. Figure 2A shows comparable spheroid growth across treatment conditions. These results indicate that H. macroloba extracts did not affect spheroid size. Figure 2B shows a significant decrease in spheroid migration. This result indicates that H. macroloba extracts may inhibit the migration of SiHa spheroid cells.

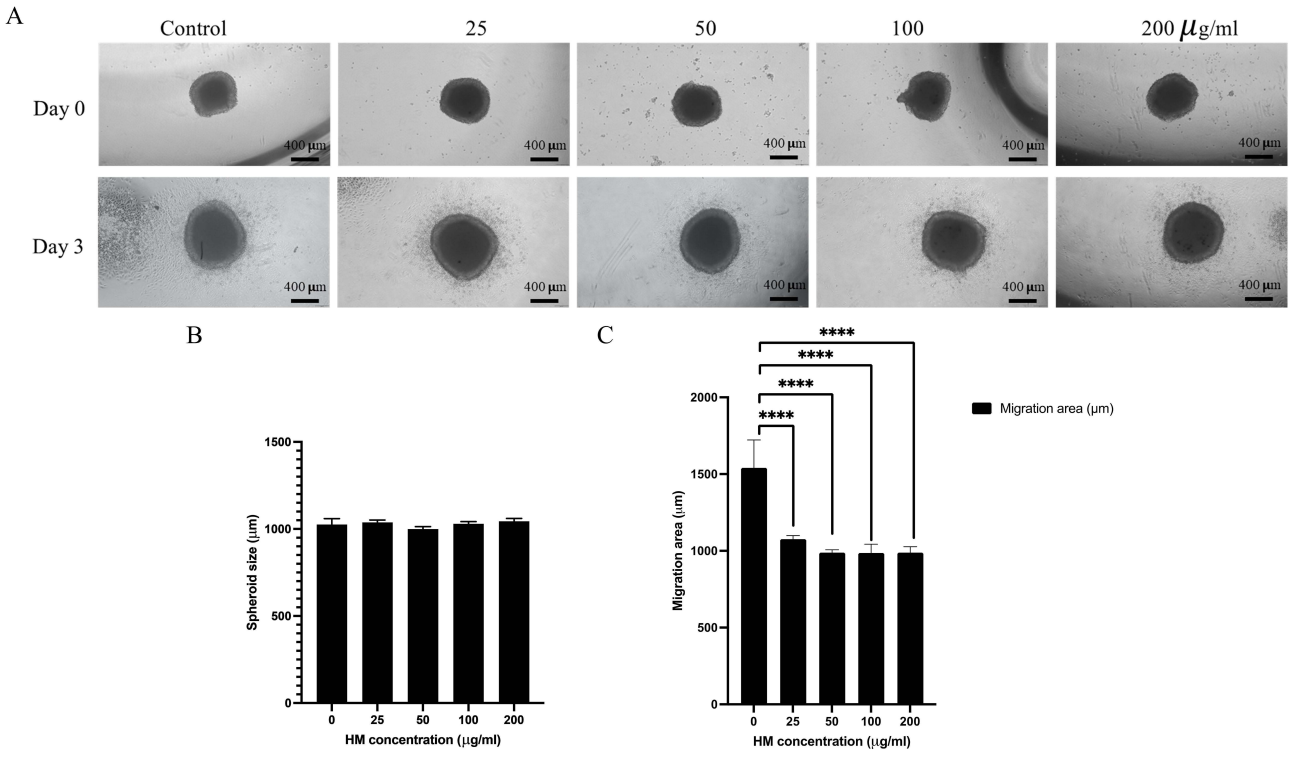

Figure 2 Effect of *Halimeda macroloba* extracts on cervical cancer spheroid. Cell morphology of SiHa spheroid after treatment for 72 h (upper panel). The migration of spheroids was observed after 72 h post-treatment (lower panel) (**A**). *H. macroloba* extracts showed no difference on spheroid size (**B**). Spheroid migration was significantly decreased (**C**). Scale bar = 400 µm. Statistical analysis was performed using the Student's *t*-test. Significance: **** $p < 0.0001$.

https://doi.org/10.2147/CMAR.S611650

H. macroloba Extracts Induced Cervical Cancer Spheroid Death

After spheroid treatment, cell viability was determined by staining the spheroids using a LIVE/DEAD cell imaging kit. Figure 3 shows the cytotoxic effects of *H. macroloba* extracts on spheroid cells. The results demonstrated a decrease in green fluorescence from calcein AM-stained viable cells, and an increase in red fluorescence from nucleic acid staining-BOBO-3 for dead cells, thereby indicating enhanced cell death in the *H. macroloba* extract-treated group compared to the control. Our results revealed that dead cells—indicated by the red fluorescent signal—were located in the center of the SiHa spheroid, while the edge of spheroids showed a green fluorescent signal—indicating living cells.

H. macroloba Extracts Induced Spheroid Death Through Caspase Activation

The mode of cell death after spheroid treatment was investigated using the ApoLive-Glo™ assay kit. Cell viability was evaluated using live cell protease activity to produce fluorescent AFC. Caspase activity was evaluated based on the cleavage of caspase, which is a substrate for luciferase (aminoluciferin). Protease activity was calculated as a percentage of viable cells. Figures 3B and C show the cell viability and caspase activity of the *H. macroloba* extracts, respectively. The results revealed a decrease in cell viability, which correlated with the LIVE/DEAD assay. These results confirmed that *H. macroloba* extracts exhibited dose-dependent cytotoxicity against SiHa spheroids. Moreover, caspase activity was measured to confirm apoptosis. We observed an increase in caspase activity in the *H. macroloba* extract-treated groups. However, caspase activity decreased slightly at 25 µg/mL and increased at 50 µg/mL. We hypothesized that this is attributed to negative feedback in the 25 µg/mL treatment group.

Proteomic Analysis Revealed Cell Death Induction Through Apoptosis and Ferroptosis Pathway

The protein expression profiles of SiHa spheroids incubated with or without *H. macroloba* extract are shown in Figure 4. The Venn diagram showed that 120 proteins were uniquely expressed in the control group (HM-0), whereas 47 proteins were uniquely expressed in the treatment group (HM-200). Gene Ontology analysis of these unique proteins revealed

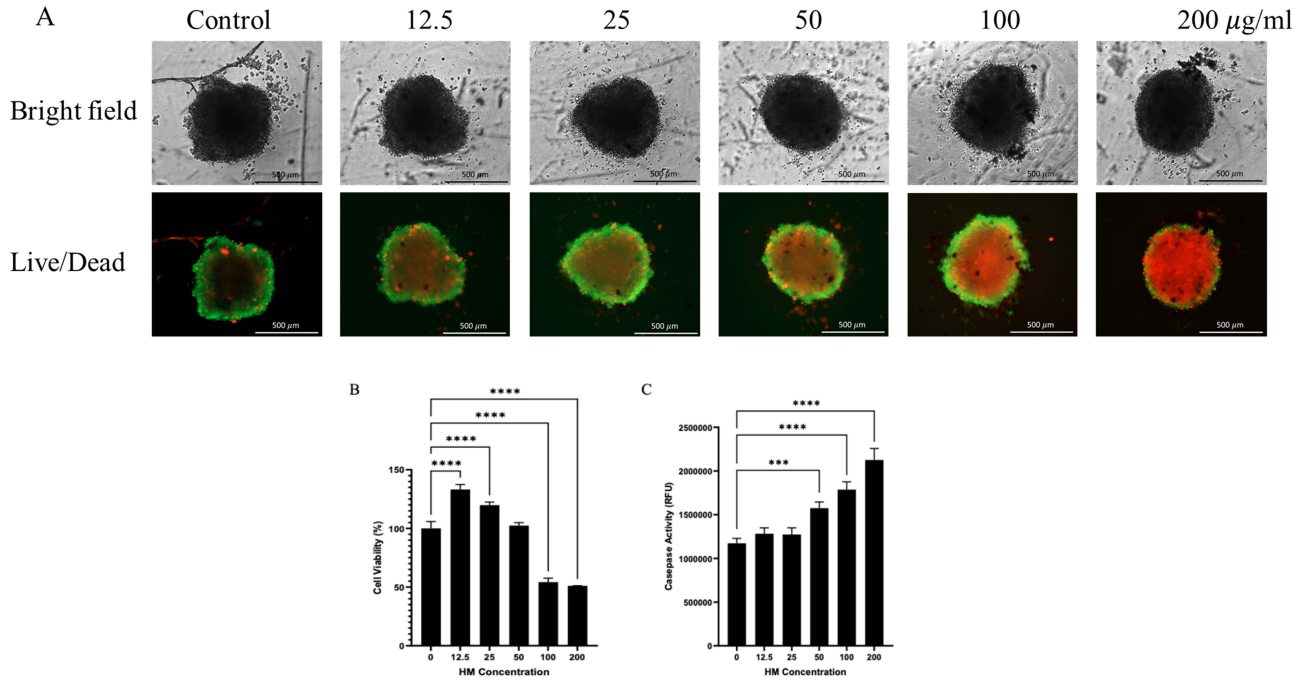

Figure 3 Cytotoxic effects of *Halimeda macroloba* extracts on cervical cancer spheroids. After treatment with *H. macroloba* extracts at various concentration for 72 h, the LIVE/DEAD staining (**A**, live = green, dead = red) of the spheroids was visualized with a LionheartFX live cell imager (10x magnification). Scale bar = 500 µm. The ApoLive-Glo™ assay was used to determine cell viability (**B**) and caspase-3/7 activity (**C**). Statistical analysis was performed using the Student's *t*-test. Significance:*** $p < 0.001$, **** $p < 0.0001$.

https://doi.org/10.2147/CMAR.S611650

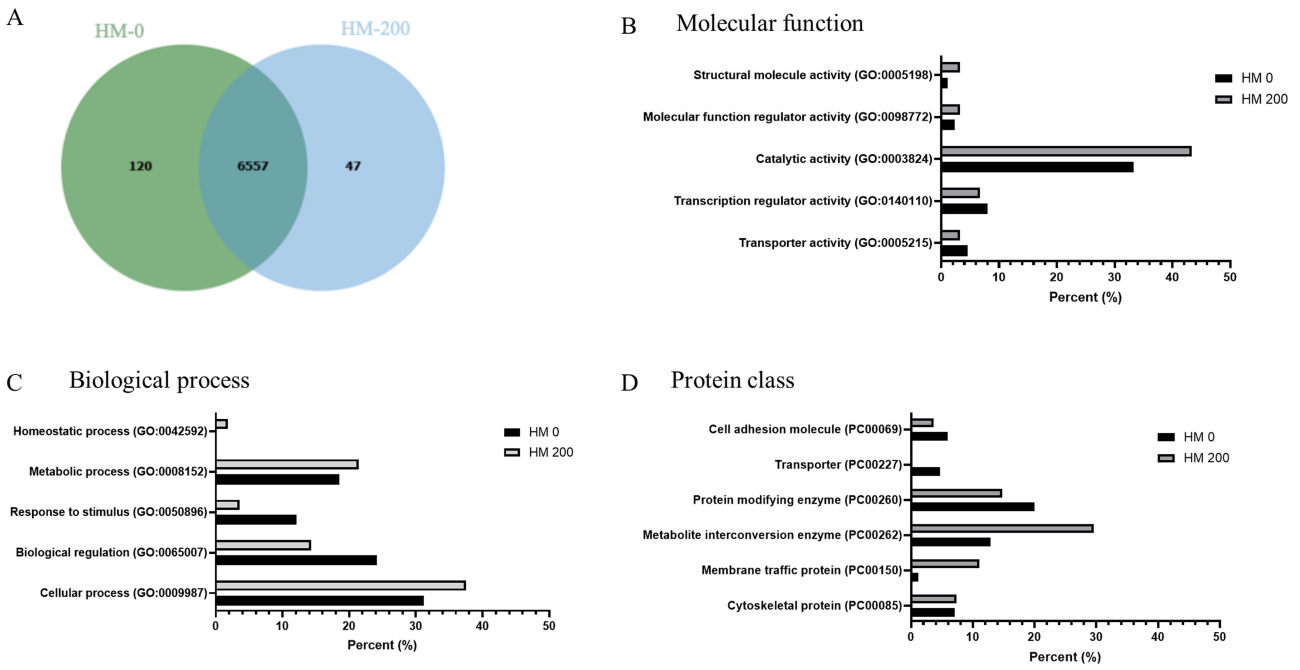

Figure 4 Proteomic data revealed protein expression changes associated with the bioactive effects of *Halimeda macroloba* extract in cervical cancer spheroids. Venn diagram of control (HM-0) and *H. macroloba* extracts (HM-200) on cervical cancer spheroid (**A**). A unique protein list in each group was subjected to the Panther database (PANTHER 19.0) to identify the molecular function using GO terms annotated (**B**), biological process (**C**), and protein class (**D**).

distinct expression patterns between the groups. In terms of MF, both groups exhibited proteins associated with structural molecular activity, MF regulation, and, most prominently, catalytic activity, with a higher percentage in the HM-200 treatment group. Additionally, transcriptional regulator and transporter activities were higher in the control group than in the treatment group. Analysis of BPs indicated that proteins involved in the response to stimuli and biological regulation were classified in the control group. Meanwhile, proteins associated with homeostatic, metabolic, and cellular processes were classified in the treatment group. Classification by protein class further demonstrated that metabolite interconversion enzymes and membrane trafficking proteins were highly expressed in the HM-200 treatment group.

Figure 5A presents a heatmap of the top 100 differentially expressed proteins, and Figures 5B and C illustrate the enrichment analyses. The heat map demonstrates a different pattern of proteins in the treatment and control groups. The dot plots in Figures 5B and C represent the enrichment of MF and BP, respectively. In the treatment group, MF enrichment included ubiquitin-related proteins, such as ubiquitin ligase, ubiquitin transferase, and ubiquitin-like modifiers, which are associated with the induction of cell death. In contrast, proteins related to microtubule and tubulin binding, as well as structural constituents, were enriched in the MF category of the control group.

Notably, proteins involved in various metabolic pathways, including retinoid, diterpenoid, terpenoid, isoprenoid, and retinol metabolism, were enriched in the BP of the treatment group. Additionally, proteins in the mitochondrial respiratory chain were enriched. This is consistent with mitochondrial disintegration leading to apoptosis and ferroptosis. Conversely, BP enrichment in the control group revealed the presence of virus-related proteins, including response to viruses, defense response to viruses, negative regulation of genome replication, and regulation of viral life cycle processes—notably those associated with human papillomavirus type 16 genome infection in SiHa cells. Table 1 lists 100 differentially expressed proteins in the control and treatment groups.

Molecular Mechanism of H. macroloba Extracts in Cervical Cancer Spheroids

The molecular mechanism of *H. macroloba* (HM) extract has previously been associated with its flavonoid constituents, which exhibit anticancer activities through modulation of multiple signaling pathways involved in cell proliferation, survival, and apoptosis. To investigate the potential molecular effects of HM treatment, the expression of proteins associated with the Akt/mTOR signaling network and apoptotic pathways was evaluated by Western blot analysis

https://doi.org/10.2147/CMAR.S611650

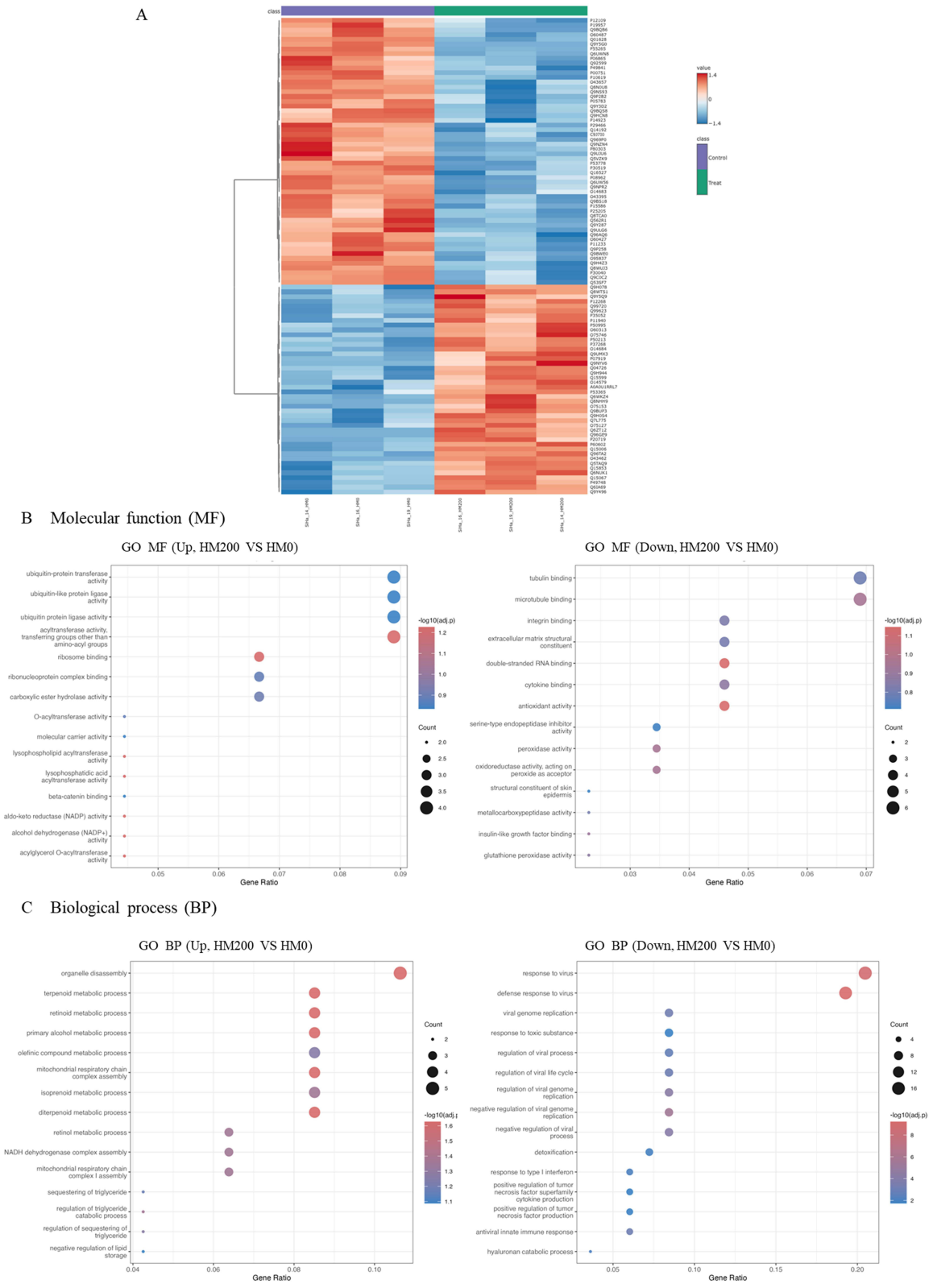

Figure 5 Heat map providing intuitive visualization of a proteomic data of control (HM-0) and *Halimeda macroloba* extracts (HM-200) treatment on cervical cancer spheroid. The top 100 of upregulated and downregulated expression in each group (**A**). Control group (HM-0) is shown in purple, while treatment group (HM-200) in shown in green. Blue represents low expression (−1.4) and red represents high expression (1.4). Enrichment analysis was performed using the clusterProfiler package. Gene Ontology (GO) enrichment was conducted for molecular function (MF), (**B**) and biological process (BP), (**C**) categories.

Table 1 List of Top 100 Proteins in Heatmap Analysis

No.	Up in Control Group		Up in Treatment Group	
	Protein ID	Protein Description	Protein ID	Protein Description
1	P12109	Collagen alpha-1(VI) chain	Q5TAQ9	DDB1- and CUL4-associated factor 8
2	P19957	Elafin	Q15853	Upstream stimulatory factor 2
3	Q9BQB6	Vitamin K epoxide reductase complex subunit 1	Q6NUK1	Mitochondrial adenyl nucleotide antiporter SLC25A24
4	O60487	Myelin protein zero-like protein 2	P98175	RNA-binding protein 10
5	Q01628	Interferon-induced transmembrane protein 3	O75153	Clustered mitochondria protein homolog
6	Q9Y5G0	Protocadherin gamma-B5	P60602	Reactive oxygen species modulator 1
7	P55265	Double-stranded RNA-specific adenosine deaminase	Q15006	ER membrane protein complex subunit 2
8	Q6UWN8	Serine protease inhibitor Kazal-type 6	P53365	Arfaptin-2
9	P00751	Complement factor B	Q96TA2	ATP-dependent zinc metalloprotease YME1L1
10	P10619	Lysosomal protective protein	O43462	Membrane-bound transcription factor site-2 protease
11	P49841	Glycogen synthase kinase-3 beta	O14579	Coatomer subunit epsilon
12	P06865	Beta-hexosaminidase subunit alpha	A0A0U1RRL7	Protein MMP24OS
13	Q92599	Septin-8	Q9NYV6	RNA polymerase I-specific transcription initiation factor RRN3
14	Q8N0U8	Vitamin K epoxide reductase complex subunit 1-like protein 1	Q9UMX3	Bcl-2-related ovarian killer protein
15	O43657	Tetraspanin-6	P07919	Cytochrome b-c1 complex subunit 6, mitochondrial
16	Q9NS93	Transmembrane 7 superfamily member 3	Q9H0S4	Probable ATP-dependent RNA helicase DDX47
17	Q9P2B2	Prostaglandin F2 receptor negative regulator	Q7L775	EPM2A-interacting protein 1
18	P05783	Keratin, type I cytoskeletal 18	O75127	Pentatricopeptide repeat-containing protein 1, mitochondrial
19	Q9Y3D2	Methionine-R-sulfoxide reductase B2, mitochondrial	Q6ZT12	E3 ubiquitin-protein ligase UBR3
20	Q9BQS8	FYVE and coiled-coil domain-containing protein 1	Q96GE9	Distal membrane-arm assembly complex protein 1
21	Q9HCN8	Stromal cell-derived factor 2-like protein 1	P20719	Homeobox protein Hox-A5
22	P14923	Junction plakoglobin	Q6WKZ4	Rab11 family-interacting protein 1
23	P29466	Caspase-1	Q8NHH9	Atlastin-2
24	Q14192	Four and a half LIM domains protein 2	Q9BUP3	Oxidoreductase HTATIP2
25	C9J7I0	UBAP1-MVB12-associated (UMA)-domain containing protein 1	P12268	Inosine-5'-monophosphate dehydrogenase 2
26	Q969P0	Immunoglobulin superfamily member 8	Q99720	Sigma non-opioid intracellular receptor 1
27	Q9NZN4	EH domain-containing protein 2	Q99623	Prohibitin-2
28	P80303	Nucleobindin-2	P35052	Glypican-1
29	Q9UJU6	Drebrin-like protein	P11940	Polyadenylate-binding protein 1
30	P53778	Mitogen-activated protein kinase 12	O75746	Electrogenic aspartate/glutamate antiporter SLC25A12, mitochondrial
31	P30519	Heme oxygenase 2	Q15067	Peroxisomal acyl-coenzyme A oxidase 1
32	O14683	Tumor protein p53-inducible protein 11	P49748	Very long-chain specific acyl-CoA dehydrogenase, mitochondrial

(*Continued*)

Table 1 (Continued).

No.	Up in Control Group		Up in Treatment Group	
	Protein ID	**Protein Description**	**Protein ID**	**Protein Description**
33	Q16527	Cysteine and glycine-rich protein 2	Q6IA69	Glutamine-dependent NAD(+) synthetase
34	P08962	CD63 antigen	Q9Y496	Kinesin-like protein KIF3A
35	Q6UW56	All-trans retinoic acid-induced differentiation factor	Q9H078	Mitochondrial disaggregase
36	Q9NPR2	Semaphorin-4B	Q8WTS1	1-acylglycerol-3-phosphate O-acyltransferase ABHD5
37	Q5VZK9	F-actin-uncapping protein LRRC16A	Q04726	Transducin-like enhancer protein 3
38	O43395	U4/U6 small nuclear ribonucleoprotein Prp3	Q9H944	Mediator of RNA polymerase II transcription subunit 20
39	Q9BS18	Anaphase-promoting complex subunit 13	Q15599	Na(+)/H(+) exchange regulatory cofactor NHE-RF2
40	P15586	N-acetylglucosamine-6-sulfatase	P50995	Annexin A11
41	P25205	DNA replication licensing factor MCM3	O60313	Dynamin-like 120 kDa protein, mitochondrial
42	Q8TCA0	Leucine-rich repeat-containing protein 20	P50213	Isocitrate dehydrogenase [NAD] subunit alpha, mitochondrial
43	Q562R1	Beta-actin-like protein 2	P37268	Squalene synthase
44	Q9Y287	Integral membrane protein 2B	O14684	Prostaglandin E synthase
45	Q9ULG6	Cell cycle progression protein 1		
46	Q96AQ6	Pre-B-cell leukemia transcription factor-interacting protein 1		
47	O60427	Acyl-CoA (8-3)-desaturase		
48	P11233	Ras-related protein Ral-A		
49	Q9P258	Protein RCC2		
50	Q9BWE0	Replication initiator 1		
51	O95837	Guanine nucleotide-binding protein subunit alpha-14		
52	Q9H4Z3	mRNA (2'-O-methyladenosine-N(6)-)-methyltransferase		
53	Q8WUJ3	Cell migration-inducing and hyaluronan-binding protein		
54	P30040	Endoplasmic reticulum resident protein 29		
55	Q9C0C2	182 kDa tankyrase-1-binding protein		
56	Q53SF7	Cordon-bleu protein-like 1		

(Figure 6 and Supplementary Figure 1). HM treatment resulted in a dose-dependent increase in p-Akt/Akt expression, whereas p-mTOR/mTOR expression was significantly reduced. These findings indicate that HM modulates components of the Akt/mTOR signaling network; however, the observed expression pattern does not support a simple inhibition of the entire pathway and may reflect the involvement of additional regulatory mechanisms. In contrast, the expression levels of apoptosis-related proteins, including Bax, cleaved caspase-3, and cytochrome c, increased in a dose-dependent manner, suggesting activation of the mitochondrial apoptotic pathway. Collectively, these results support the pro-apoptotic activity of HM extract in cervical cancer cells, while further studies are required to elucidate the precise relationship between Akt activation and mTOR suppression.

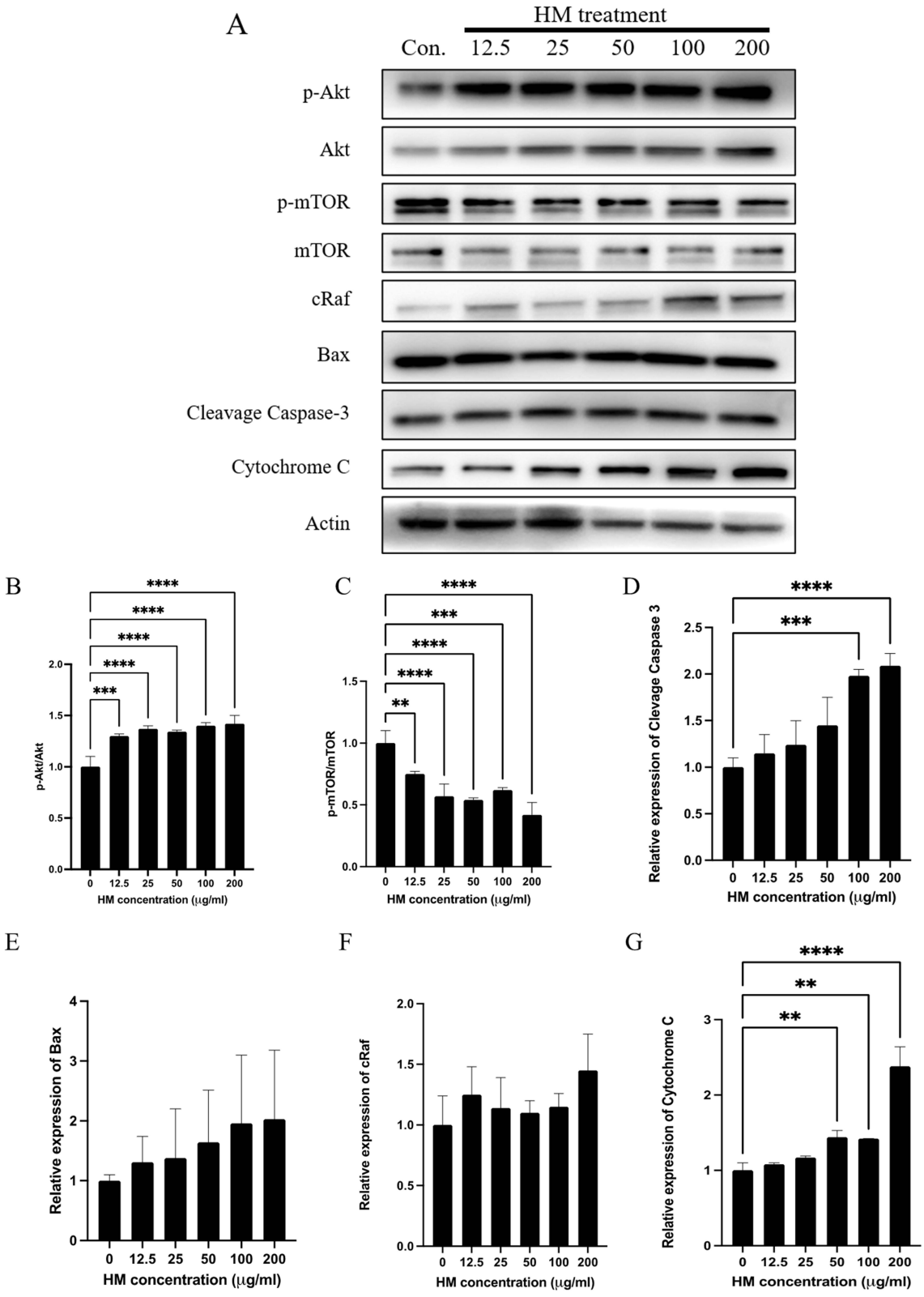

Figure 6 Effect of *Halimeda macroloba* extracts on the Akt, mTOR, and apoptosis pathway. The spheroids were treated with *H. macroloba* extracts at various concentration for 72 h. After incubation, the spheroids were collected and lysed. (**A**) The proteins were loaded on SDS-PAGE, and those of interest were examined by Western blot analysis. Actin was used as internal control. The quantitative proteins of interest, including (**B**) p-Akt/Akt, (**C**) p-mTOR/mTOR, (**D**) cleavage-Caspase 3, (**E**) Bax, (**F**) cRaf, and (**G**) Cytochrome C, were normalized to actin band intensity. Data are shown as the mean ± SD of triplicate experiments. Statistical analysis was performed using Student's *t*-test. Significance: ** $p < 0.01$ compared with the control. *** $p < 0.001$ compared with the control. **** $p < 0.0001$ compared with the control.

https://doi.org/10.2147/CMAR.S611650

Discussion

Various phytochemical constituents, including terpenoids, alkaloids, steroids, saponins, phenolic compounds, and flavonoids, have been identified in the crude extracts of *H. macroloba*. Flavonoids and steroids are considered potential bioactive compounds associated with anticancer mechanisms. The anticancer activity of these metabolites involves the generation of reactive oxygen species (ROS), which leads to mitochondrial damage, caspase activation, and cytochrome c release, all of which ultimately result in apoptosis. Our findings demonstrated that *H. macroloba* extracts exhibited cytotoxic potential against SiHa cervical cancer spheroid cells. Initially, Cytotoxicity was assessed by measuring spheroid size; however, no significant differences were observed among the treatment groups. This result may be explained by the loose aggregation morphology of the SiHa spheroids. Notably, LIVE/DEAD assays revealed that cell death predominantly occurred in the spheroid core, whereas cells in the outer layer remained viable. This observation is consistent with the structural characteristics of SiHa spheroids, which typically exhibit a flat morphology with a densely packed center and a less compact periphery.[14] Based on these findings, we propose that the *H. macroloba* extract exerts stronger effects under hypoxic conditions than under normoxic conditions. Similar anticancer properties have been reported in related Halimeda species. Methanolic extracts of *Halimeda tuna* demonstrated anticancer activity against HeLa cervical cancer cells and A549 lung cancer cells.[17,18] Additionally, studies on breast, colorectal, and liver cancers have shown the cytotoxic activity of methanolic *H. macroloba* extracts, supporting their potential antiproliferative effects.[19] Furthermore, *Halimeda gracilis* extract induced cytotoxicity in MDA-MB-231 breast cancer cells through ROS overproduction, mitochondrial dysfunction, and apoptosis.[2] Previous studies have also reported that *H. macroloba* extracts exhibit diverse therapeutic activities, including antioxidant, antiplasmodial, α-glucosidase inhibitory, antimicrobial, antiproliferative, and wound-healing effects.[5] Investigations of its antioxidant activity identified flavonoids and steroids as major active constituents.[6,10] However, the molecular mechanisms underlying these anticancer effects remain poorly understood. In this study, we investigated the molecular effects of *H. macroloba* extract on SiHa spheroids while focusing on the Akt/mTOR and apoptotic pathways, which are established targets of its bioactive compounds. Proteomic analysis further revealed enrichment of proteins associated with mitochondrial function and organelle disassembly in the treatment group, suggesting the activation of apoptosis-related pathways and the possible involvement of ferroptosis-associated mechanisms. Proteins uniquely expressed in the *H. macroloba* extract-treated group were enriched for higher catalytic activity, metabolic processes, and metabolite interconversion enzymes than in the control group. The proteins in the heatmap were highly expressed in the treatment group, including the ROS modulator 1 (P60602 and ROMO1), which plays a role in inducing oxidative DNA damage and oxidative stress.[20] This leads to the expression of apoptosis-related proteins, such as the Bcl-2-related ovarian killer protein (Q9UMX), cytochrome b-c1 complex subunit 6, mitochondria (P07919), and E3 ubiquitin-protein ligase UBR3. The key anticancer activity of ROMO1 is its role as a ROS-regulating protein that can increase the activation of c-Jun N-terminal kinase, thereby leading to apoptotic cell death. Enrichment analysis of molecular functions demonstrated a high gene ratio for acyltransferase activity and various ubiquitin ligase and transferase activities in the *H. macroloba* extract-treated group. Additionally, enrichment analysis of BPs revealed various metabolic processes in the *H. macroloba* extract treatment group, including retinoids, diterpenoids, terpenoids, and olefinic compounds, which may play a key role in the anticancer activity of cervical cancer spheroids.

Notably, our results revealed a significant downregulation of mTOR accompanied by a dose-dependent increase in apoptotic proteins, supporting the role of both apoptotic and ROS-mediated pathways in the cytotoxic effects of *H. macroloba* extract.

Conclusion

H. macroloba extract demonstrated significant cytotoxic potential against cervical cancer spheroids, with evidence suggesting the involvement of apoptosis-related pathways and possible ferroptosis-associated mechanisms. The enhanced effects observed in spheroid cultures may be associated with microenvironmental characteristics of the 3D spheroid model, including limited oxygen diffusion, together with proteomic enrichment of mitochondrial dysfunction- and organelle disassembly-related pathways. Consistent with previous reports on related *Halimeda* species and other cancer models, these findings support the potential of *H. macroloba* as a source of bioactive compounds with anticancer activity.

However, additional studies incorporating specific molecular markers and functional validation are required to confirm the involvement of ferroptosis-related pathways, clarify the underlying cell death mechanisms, and determine the role of hypoxia-related effects Furthermore, isolation and characterization of the active compounds, together with evaluation of their bioavailability and pharmacokinetic properties, as well as validation in preclinical in vivo models, are necessary before clinical translation can be considered. This study is also limited by the evaluation of only short-term treatment responses in the 3D spheroid model; therefore, further investigation of long-term effects is warranted. In addition, while L929 and HEK-293 cells were used as representative non-cancerous controls to evaluate general cytotoxicity and safety, future studies should include immortalized normal cervical epithelial cells and corresponding 3D spheroid models to further assess tissue-specific selectivity and compare the effects of *H. macroloba* extract on normal and malignant cervical tissues within a more physiologically relevant microenvironment. Collectively, this study provides preliminary evidence supporting the anticancer potential of *H. macroloba* extracts against cervical cancer.

Acknowledgments

The authors gratefully acknowledge the Seaweed and Seagrass Research Unit team, Prince of Songkla University, who assisted us with fieldwork on *H. macroloba* extract preparation from Parinuch Chumkaew, Faculty of Science and Industrial Technology, Prince of Songkla University, Surat Thani Campus, and Surat Thani. The authors acknowledge the use of an AI platform (ChatGPT) for grammar checks and English language editing.

Funding

This research was funded by the National Science and Research and Innovation Fund (NSRF), Prince of Songkla University (SCI6801020S) and the Postdoctoral Fellowship Program from the Faculty of Medicine, Prince of Songkla University.

Disclosure

The authors report no conflicts of interest in this work.

References

1. Hawas UW, Husain S, El-Kassem LTA. Biochemical composition and biological properties of some red and green algae from the Saudi Red Sea coast. *Thalassas*. 2025;41(2):104. doi:10.1007/s41208-025-00856-w
2. Ramalingam V, Narendra Kumar N, Harshavardhan M, et al. Chemical profiling of marine seaweed *Halimeda gracilis* using UPLC-ESI-Q-TOF-MSE and evaluation of anticancer activity targeting PI3K/AKT and intrinsic apoptosis signaling pathway. *Food Res Int*. 2022;157:111394. doi:10.1016/j.foodres.2022.111394
3. Cremen MCM, Huisman JM, Marcelino VR, Verbruggen H. Taxonomic revision of *Halimeda* (Bryopsidales, Chlorophyta) in south-western Australia. *Aust Syst Bot*. 2016;29(1):41–54. doi:10.1071/SB15043
4. Kooistra WHCF, Coppejans EGG, Payri C. Molecular systematics, historical ecology, and phylogeography of *Halimeda* (Bryopsidales). *Mol Phylogenet Evol*. 2002;24(1):121–138. doi:10.1016/S1055-7903(02)00221-X
5. Saber AA, Rashedy SH, Rushdi MI, et al. Insights into the phytochemical and pharmacological natural products of the green macroalga *Halimeda* (Chlorophyta). *Nat Prod Commun*. 2025;20(3). doi:10.1177/1934578X251331137
6. Widowati R, Handayani S, Suprihatin ILR. Phytochemicals and antioxidant of methanol extract of *Gracilaria salicornia*, *Halimeda gracilis*, *Halimeda macroloba*, and *Hypnea asperi* from Tidung Island coastal region. *Eur J Mol Clin Med*. 2021;8:1–12.
7. Navakanitworakul R, Nittayaboon K, Chumkaew P, Phetcharat S, Mayakun J. Phytochemical screening and cytotoxic activities of *Enhalus acoroides* (L.f.) Royle and *Halimeda macroloba* Decaisne on cervical cancer cell lines. *Trop J Pharm Res*. 2025;23(12):2053–2057. doi:10.4314/tjpr.v23i12.10
8. Mayakun J, Prathep A. Calcium carbonate productivity by *Halimeda macroloba* in the tropical intertidal ecosystem: the significant contributor to global carbonate budgets. *Phycol Res*. 2019;67(2):94–101. doi:10.1111/pre.12361
9. Mayakun J, Liao CP, Liu SL. The standing stock and CaCO 3 contribution of *Halimeda macroloba* in the tropical seagrass-dominated ecosystem in Dongsha Island, the main island of Dongsha Atoll, South China Sea. *J Mar Biol Assoc UK*. 2020;100(8):1219–1227. doi:10.1017/S0025315420001113
10. Nazarudin MF, Yasin ISM, Mazli NAIN, et al. Preliminary screening of antioxidant and cytotoxic potential of green seaweed, *Halimeda opuntia* (Linnaeus) Lamouroux. *Saudi J Biol Sci*. 2022;29(4):2698–2705. doi:10.1016/j.sjbs.2021.12.066
11. Wongpratate M, Bumrungthai S. Cervical cancer in Thailand: 2023 update. *Obstet Gynecol Sci*. 2024;67(3):261–269. doi:10.5468/ogs.23277
12. Tewari KS. Cervical cancer. *N Engl J Med*. 2025;392(1):56–71. doi:10.1056/NEJMra2404457
13. Rocha DHA, AML Seca, Pinto DCGA. Seaweed secondary metabolites in vitro and in vivo anticancer activity. *Mar Drugs*. 2018;16:410. doi:10.3390/md16110410
14. Molika P, Leetanaporn K, Chiangjong W, Choochuen P, Navakanitworakul R. Proteomic analysis reveals cadherin, actin, and focal adhesion molecule-mediated formation of cervical cancer spheroids. *Cells*. 2024;13(23):2004. doi:10.3390/cells13232004

15. Potriquet J, Laohaviroj M, Bethony JM, Mulvenna J. A modified FASP protocol for high-throughput preparation of protein samples for mass spectrometry. *PLoS One*. 2017;12(7):e0175967. doi:10.1371/journal.pone.0175967
16. Demichev V, Messner CB, Vernardis SI, Lilley KS, Ralser M. DIA-NN: neural networks and interference correction enable deep proteome coverage in high throughput. *Nat Meth*. 2020;17(1):41–44. doi:10.1038/s41592-019-0638-x
17. Gazali M, Husni A, Sukmadewi AP, et al. Anticancer activity of marine macroalgae *Halimeda tuna* from Aceh waters against cervical cancer cells. *J Fish Environ*. 2024;48:120–131.
18. Husni A, Gazali M, Nurjanah N, Syafitri R, Matin A, Zuriat Z. Cytotoxic activity of green seaweed *Halimeda tuna* methanolic extract against lung cancer cells. *J Multidiscip Appl Nat Sci*. 2024;4(1):16–29. doi:10.47352/jmans.2774-3047.172
19. Nazarudin MF, Isha A, Mastuki SN, et al. Chemical composition and evaluation of the α-glucosidase inhibitory and cytotoxic properties of marine algae *Ulva intestinalis, Halimeda macroloba*, and *Sargassum ilicifolium*. *Evid Based Complement Alternat Med* 2020;2020(1):2753945. doi:10.1155/2020/2753945
20. Amini MA, Talebi SS, Karimi J. Reactive oxygen species modulator 1 (ROMO1), a new potential target for cancer diagnosis and treatment. *Chonnam Med J*. 2019;55(3):136–143. doi:10.4068/cmj.2019.55.3.136